Evaluation of heterogeneous aquifers in hard rocks from resistivity sounding data in parts of Kalmeshwar taluk of Nagpur district, India

Dewashish Kumar*, S. N. Rai, S. Thiagarajan and Y. Ratna Kumari

CSIR-National Geophysical Research Institute, Hyderabad 500 007, India

Interpretation of vertical electrical sounding (VES) data coupled with the estimation of coefficient of anisotropy (λ) in parts of Kalmeshwar taluk, Nagpur district, Maharashtra, India has yielded vital information on the characteristics of subsurface basaltic aquifers. The coefficient of anisotropy estimated at 22 sites from VES data has shown variation between 1 and 1.87, which in turn reveals the anisotropic character of the basaltic aquifers. The estimated fracture porosity from the interpreted parameters and specific conductance of groundwater within the region varies from 0.007% to ~2%, indicating different degrees of water saturation within the basaltic flows. The interpreted true resistivity ~10–35 Ω.m corroborates well with the zones of high porosity and λ further substantiates the presence of exploitable groundwater resources within the region.

Keywords: Anisotropy, hard rock aquifers, fracture, porosity, vertical electrical sounding.

FRACTURES act as important conduits for groundwater flow in hard rocks. The flow of groundwater through a fracture network is largely influenced by hydraulic anisotropy resulting from the geometry and orientation of the fractures. The preferential strike of fracture zones makes the host rock both electrically and hydraulically anisotropic, whereas variation in the size and opening of fractures causes heterogeneity[1]. The identification and characterization of fractures is important in rocks having low primary (or matrix) porosity because the bulk porosity and permeability are determined mainly by the intensity, orientation, connectivity, aperture and infill of fracture systems[2]. The hydraulic conductivity of fracture systems generally ranges over several orders of magnitude. It is assumed that the principal directions of hydraulically conductive fracture measured from electrical anisotropy are inferred from the measured electrical anisotropy since both current flow and groundwater are channelled through fractures in the rock. The coefficient of anisotropy (λ), a unique and dimensionless number, is a measure of the degree of inhomogeneity arising from fracturing, faulting, jointing and weathering in different varieties of hard rocks. A geologic section differs from a geoelectric section when the boundaries between geologic layers do not coincide with those between layers characterized by different resistivities[3–6]. Hard-rock aquifers are potential only when the fractures are interconnected and extend in all the directions. Such fracture systems are reflected by large values of λ (ref. 7). Ben and Onwuemesi[8] determined and characterized the anisotropic properties of fractures in Presco campus of Ebonyi State University, Nigeria to evaluate the groundwater development and flow within the area. They showed that a higher coefficient of anisotropy implies higher permeability anisotropy. A similar study for groundwater potential evaluation using electrical resistivity method in a typical basement complex area of Nigeria has been carried out by Ayolabi *et al.*[9], who have demonstrated the significance of coefficient of anisotropy in groundwater potential evaluation.

It is necessary to delineate lithologic units, which are favourable for groundwater accumulation and the secondary parameters using resistivity and thickness such as longitudinal unit conductance (S_t), transverse unit resistance (T_t), longitudinal resistivity (ρ_L), transverse resistivity (ρ_t) and the coefficient of anisotropy (λ) – complementary to the fundamental parameters, namely resistivity and thickness of the layered earth. Nevertheless, when resistivity methods are used, limitations can be expected if ground inhomogeneities and anisotropy are present[10]. Anisotropy in a geological body arises due to several reasons and is usually in the range 1.1–2 (refs 5, 11). Forty-five vertical electrical sounding (VES) measurement have been made in water-scarce area of Nagpur district, Maharashtra covering different villages with different geomorphic units. Both qualitative and quantitative interpretations of the VES data were carried out for groundwater prospecting, evaluation and exploration. The study reveals the presence of hidden source of groundwater within the traps in weathered, fractured basalt and at the same time in parts in the Gondwana Formation below the Deccan traps. The result of standard resistivity inversion from VES data suggests the potential groundwater-bearing zones in the studied region[12]. In general, the saturated, weathered and fractured/jointed zone constitutes the main aquifer unit studied by various workers[13–16].

*For correspondence. (e-mail: dewashishkumar@ngri.res.in)

Table 1. Regional stratigraphy of the Deccan basalt region of the study area

Recent to Quaternary	Alluvial, black cotton soil and weathered formation
Deccan basalt lava flows (Cretaceous to Eocene)	Vesicular and massive basalt with intervening intertrappeans
Lameta beds (infratrappeans)	Thin sedimentary sequences
Gondwana	Sandstone of upper Kamthi Group

In the study region groundwater occurs under unconfined conditions at shallow depths in weathered/fractured mantle, in semi-confined to confined conditions in intertrappeans and vesicular beds, between two massive basalt beds and in the joints and fractured zones of massive basalts at greater depths. Groundwater withdrawal for irrigation and domestic uses is mostly from dugwells with depths ranging from ~10 to 15 m bgl penetrating up to the bottom of the weathered/fractured rock formations. Because of increasing trend in the utilization of groundwater mostly for irrigation and domestic purposes, the groundwater resources at shallower depths have been overexploited, which makes groundwater levels plummet and thus there is meagre water preserved in the weathered zones. Most of dugwells become dry during the onset of summer. Therefore, there is need for delineation of deeper and potential aquifer zones in the fractured part of the basalt at greater depths to meet the ever-increasing demand of water supply and at the same time judiciously manage this precious natural resource for safe and secured availability of groundwater in future. VES using Schlumberger configuration proved to be a useful and versatile technique for mapping the depth and thickness of aquifers[16,17–22] on the basis of surface measurement of the apparent resistivity data and their interpretation in terms of hydrogeology[16,21,23–31]. VES was carried out with a maximum current electrode spacing (*AB*) of 600 m for delineation of deeper aquifers in the form of intertrappeans/vesicular formation within the traps, in addition to the shallower aquifers and also for understanding the subsurface geoelectric layers, anisotropy behaviour, water saturation variation and for future groundwater development and management.

Geology and hydrogeology

Geologically, the area under study is underlain by Deccan traps of about 65 million years of age. Groundwater is being pumped from the bottom of the weathered, fractured and highly fractured saturated formations overlying the massive Deccan traps and at some places abundant water is available below the Deccan traps in sedimentary sequence. The low primary porosity of basalts suggests poor groundwater transmission and storage capabilities; however, the development of secondary porosity by fracturing and faulting leads to increase in the permeability of the fractured basalt. The present demand of groundwater both for drinking and irrigation purposes is much more in the area and this is often met from the deeper potential aquifer(s) only. The regional stratigraphy of the area is depicted in Table 1 to facilitate better understanding of the regional hydrogeology[32]. Each lava flow generally consists of porous vesicular basalt overlying the non-porous massive basalt. Intertrappean in association with the adjoining vesicular basalt unit forms good aquifers and shows high porosity. At some places red bole bed is found as intertrappeans. Clayey bed after being baked from the heat of lava flow is transformed to red bole bed. Massive basalt and red bole beds do not permit movement of groundwater and act as impermeable beds and hence they do not form good aquifers. Deccan traps is underlain by Lameta beds (infratrappeans), which are compact, clayey and poor in permeability and this is followed by Gondwana sediments, which are highly porous and permeable with copious amount of water reserve in the present geological setting.

Study area

The area under study is a part of Chandrabhaga river basin underlain by Deccan traps and lies within the geographical coordinates between 78°46′–78°53′E long. and 21°12′–21°15′N lat., covering an area of about 120 sq. km (Figure 1). Major part of the area under study lies in the Kalmeshwar taluk, Nagpur district. It is bounded by Chandrabhaga river in the north, while the Saptdhara river flows in the south. The Deccan traps are overlain by a thin cover of alluvial soil of varying thickness ranging from ~0.5 to 2 m with dendritic system of drainage pattern. Near-surface layer is alluvial soil and is underlain by weathered and fractured basalts followed by beds of Deccan trap of different lava flows separated by intertrappean beds of chert, cherty limestone and clay. The intertrappeans are deposited during the interval of two consecutive lava flows. Each layer of the trap is composed of vesicular basalt formation on top and compact basalt formation below. Intertrappean together with the vesicular basalt forms the groundwater potential zones between two compact basalt layers. Such area generally shows high fracture porosity values. A map of the study area with locations of electrical sounding (VES) sites and their number is shown in Figure 1.

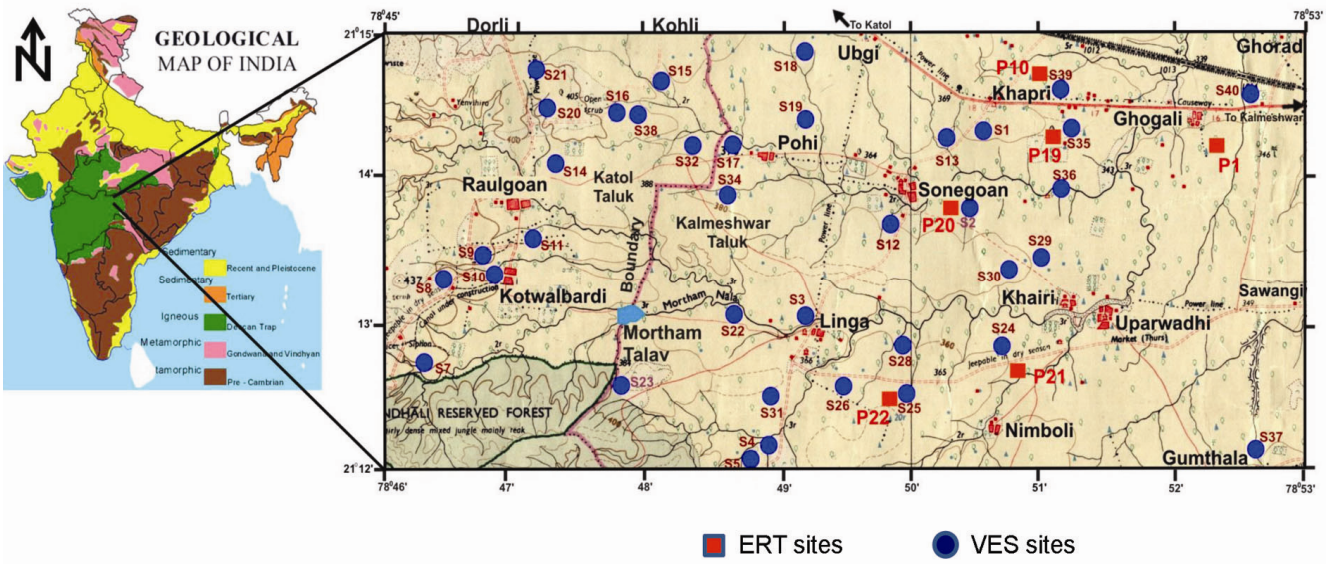

Figure 1. Location map of the study area with vertical electrical sounding (VES) sites (the geological map of India is taken from www.mapsofindia.com/maps/India/geological).

Materials and methods

Resistivity data analysis and interpretation

The electrical resistivity measurements were carried out using DC resistivity meter (Terra Science) and its accessories. At the field site VES method employing Schlumberger configuration was deployed to obtain the field resistivity data. The current electrode spread ($AB/2$) length used varied between 1.5 m and 600 m depending on the accessibility in the area, human settlements and other infrastructural masts, which sometimes posed barriers to the linear electrical resistivity profile arrangement. The measured apparent resistivity (ρ_a) field data are plotted on a double log graph paper with a modulus of 62.5 mm in an ordinate versus abscissa coordinate system as measured apparent resistivity (ρ_a) against the half current electrode separation ($AB/2$). The sounding curve so plotted shows the qualitative nature of the sounding for a given sounding position. This sounding curve reveals important subsurface information, viz. hydrogeological scenario, resistive basement, thickness of resistive layers and anisotropic condition if the data interpretation is done judiciously. The initial layer parameters/model from the field VES curve can be derived by full and partial curve matching techniques[33–35]. These geoelectrical parameters are fine-tuned by subjecting the field data to inverse numerical modelling. In the present study the quantitative interpretation of the field data was carried out with the help of RESIST[36], which optimizes the layer parameters and finally to achieve the true subsurface resistivity and thickness of the geoelectrical model. The inversion used in the program is an iterative method that successively improves the initial given model (initially guessed layer parameters, viz. resistivity and thickness or those obtained by curve matching technique), until the root mean square (RMS) error between the measured and calculated resistivities is minimum (within acceptable limit) and the parameters (namely, model resistivity and thickness of each layer) are stable with respect to a reasonable change in the model parameters, i.e. the iterative change in layer parameter is continued till the RMS error is less than a fixed limit or there is no further change in the layer parameters[21]. Here, three VES field data curves are presented, namely at S10, S22 and S40 along with the inverted model results (Figures 2 and 3). The observed and computed curves at all the three soundings are shown along with the RMS error values, which reflect the data quality and convergence of the model results. These model curves depict the quantitative interpretation and knowledge about the subsurface layer parameters, i.e. resistivity and thickness (Figures 2 and 3). The prescribed model layer parameters at S10, S22 and S40 are given in Table 2. Resistivity and thickness values so obtained served as the primary parameters that were later used to determine the secondary geoelectric parameters that characterize the vertical and horizontal dimension of the geoelectric layers through which the current penetrated.

The results of VES data in the area of study are verified by drilling a borehole near the VES site in order to confirm the interpretation of the inverted data. The lithological data are collected and calibrated with the VES model results at sounding S10 and S2 (Figures 2 and 4). Comparison of the VES results with the borehole lithologs is presented in Figures 2 and 4, which show lithological variation with depth with different resistivity characteristics of the various litho units.

Dar Zarrouk parameters for aquifer characteristics

In general, a geoelectrical earth section constructed from the analysis of VES data does not coincide with the corresponding geological section. Layers of different lithology or age or both may have the same resistivity and they form a single geoelectrical layer. Anisotropy of the subsurface layers is another factor, which would introduce errors in the estimates of true resistivity and depth in the interpretation of VES curves, especially in hard-rock regions due to the presence of inherent heterogeneity and complexity in structure. Maillet[37] introduced secondary resistivity parameters, namely transverse resistance (T), longitudinal conductance (S) and coefficient of anisotropy (λ), which helps in interpreting the subsurface geology/hydrogeology with less ambiguity. These parameters are determined at 22 selected VES sites where one or two sites represent the location in each direction of the study area. These are significant in understanding the subsurface geoelectric structure, basement nature and thickness variation, etc. for solving the hydrogeological

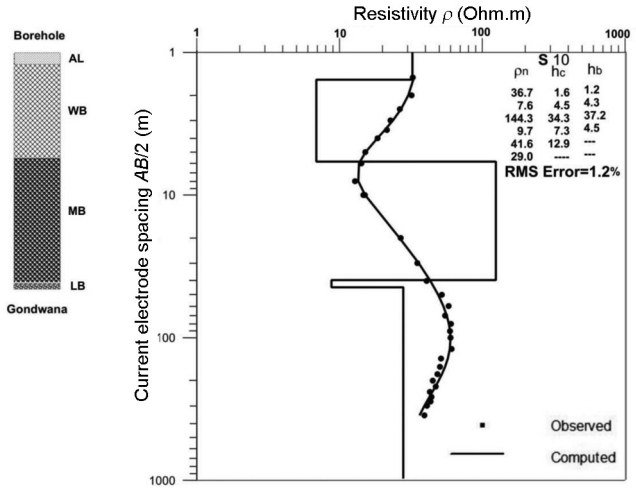

Figure 2. Interpretation of VES-S10 data (dots represent the field data and smooth line represents the computed curve) along with model layer parameters (after Rai *et al.*[22]). Lithological classification of the borehole data: AL, Alluvium; WB, Weathered basalt; MB, Massive basalt; LB, Lameta bed.

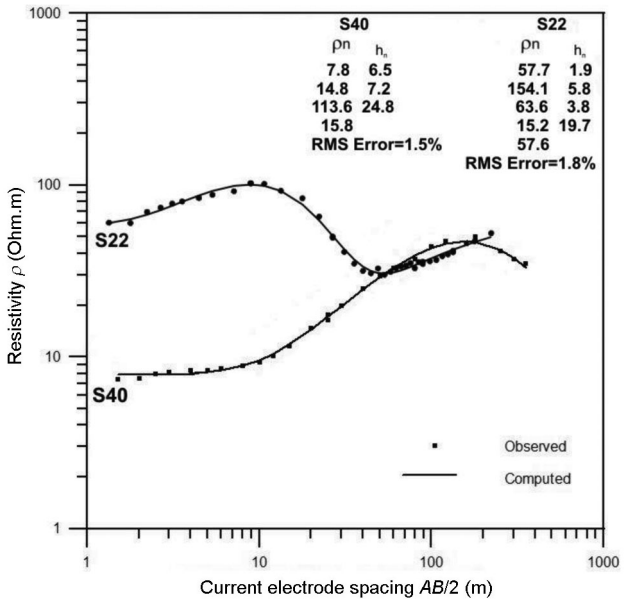

Figure 3. Interpretation of VES-S22 and S40 data (filled circle and square represent field data and smooth line represents the computed curve) along with model layer parameters.

Table 2. The prescribed model layer resistivity parameters at the sounding points, namely at S10, S22 and S40. This reflects the vertical variation of resistivity and thickness with depth in the study area

Layer	Resistivity (ρ; in Ω.m)	Thickness (h; in m)
VES at S10		
1	36.7	1.6
2	7.6	4.5
3	144.3	34.3
4	9.7	7.3
5	41.6	12.9
6	29.0	
VES at S22		
1	57.7	1.9
2	154.1	5.8
3	63.6	3.8
4	15.2	19.7
5	57.6	
VES at S40		
1	7.8	6.5
2	14.8	7.2
3	113.6	24.8
4	15.8	

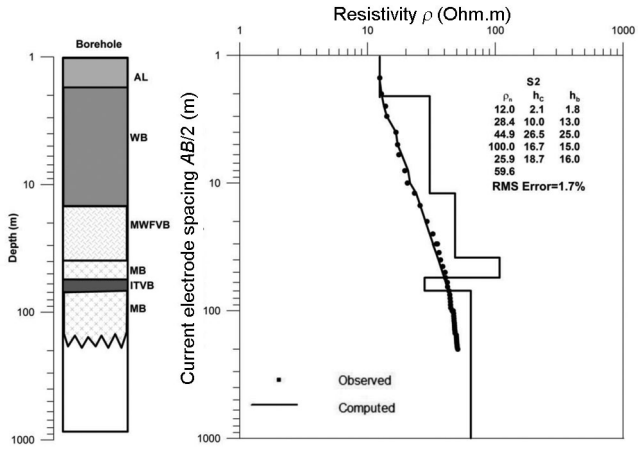

Figure 4. Interpretation of VES-S2 data (dots represent the field data and smooth line represents the computed curve) along with model layer parameters (after Rai *et al.*[12]). Lithological classification of the borehole data: AL, Alluvium; WB, Weathered basalt; MWFVB, Moderately weathered fractured vesicular basalt; MB, Massive basalt; ITVB, Water-saturated intertrappeans and vesicular basalt.

problems[5,38,39]. The graphical procedures to calculate these parameters are available in the literature[3,40,41]. In the present study the secondary resistivity parameters, namely T, S and λ as well as the longitudinal resistivity (ρ_L) and transverse resistivity (ρ_t) were estimated at 22 VES sites in order to study the anisotropy nature within the hard rock region for groundwater prospecting.

Coefficient of anisotropy and interpretation

The anisotropy coefficient (λ) is calculated from two geoelectric fundamental parameters (layer resistivity, ρ and thickness, h) as demonstrated by earlier workers[3,5]. Considering a geoelectric section of n layers with a unit cross-sectional area (Figure 5), the total longitudinal conductance S for all the possible layers for a given VES curve is given by the linear summation equation: That is, for n layers, the total longitudinal unit conductance is given by[5]

$$S = \sum_{i=1}^{n} \frac{h_i}{\rho_i} = \frac{h_1}{\rho_1} + \frac{h_2}{\rho_2} + \cdots + \frac{h_n}{\rho_n}, \quad (1)$$

while the total transverse unit resistance is defined as

$$T = \sum_{i=1}^{n} h_i \rho_i = h_1\rho_1 + h_2\rho_2 + \cdots + h_n\rho_n. \quad (2)$$

Using eq. (1), the average longitudinal resistivity for a given VES curve is given by

$$\rho_L = \frac{H}{S} = \frac{\sum_{i=1}^{n} h_i}{\sum_{i=1}^{n} \frac{h_i}{\rho_i}}. \quad (3)$$

And the average transverse resistivity using eq. (2) is defined as

$$\rho_t = \frac{T}{H} = \frac{\sum_{i=1}^{n} h_i \rho_i}{\sum_{i=1}^{n} h_i}, \quad (4)$$

and combining the above equations the anisotropy is defined as

$$\lambda = \sqrt{\frac{\rho_t}{\rho_L}}. \quad (5)$$

The parameters T and S (defined as transverse resistance and longitudinal conductance respectively) play an important role in the interpretation of sounding data[4]. These are called the Dar Zarrouk parameters[4,37].

From eqs (1) to (5), the coefficient of anisotropy is estimated along with the secondary geoelectric parameters. The estimated value of coefficient of anisotropy is shown in Figure 6. The estimation shows that the total longitudinal conductance varies from 0.1927 to 2.7089 Ω^{-1} in the area. The qualitative use of this parameter is to demarcate changes in total thickness of low resistivity materials[39]. The total transverse resistance ranges from 540.1 to 13,115.8 $\Omega.m^2$, which gives information both about the thickness and resistivity of the area. The average longitudinal resistivity calculated from sounding curves ranges from 16.99 to 197.69 Ω.m in the area, which helps in calculating the total depth H to the high resistivity bedrock and the average transverse resistivity varies from 17.09 to 247.86 Ω.m, which clearly shows that it is more than the average longitudinal resistivity. This indicates

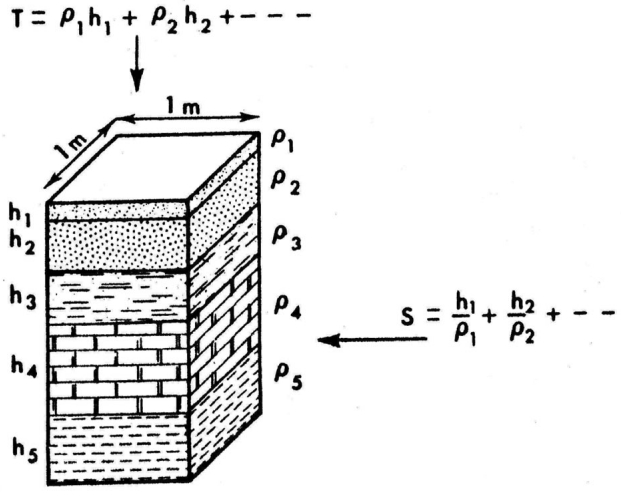

Figure 5. Representation of n-layer prism of unit cross-section showing different geoelectric-parameters in a rock mass. Columnar prism used in defining geoelectric parameters of a section. Patterns are arbitrary. ρ is the resistivity, h the thickness, S the total longitudinal conductance and T is the total transverse resistance.

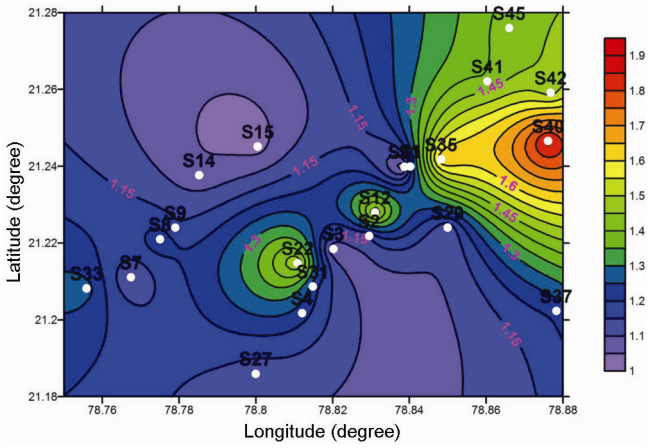

Figure 6. Map showing the variation of coefficient of anisotropy (λ) signifying fracture anisotropy in a basaltic rock formation.

that the true resistivity normal to the plane of stratification (stratified rock like Deccan basalt) is greater than the true resistivity parallel to the plane of stratification. Based on these estimates it was found that the coefficient of anisotropy λ ranges from 1.0027 to 1.8702, which depicts the true variation of the anisotropic character of rock formations. The area with high values of λ suggests that the fracture system must have extended in all the directions with different degrees of fracturing, which had greater water-holding capacity from different directions of the fracture(s) within the rock resulting in higher porosity. At the same time, unidirectional fracture may not produce good yield of water and such areas show low values of λ. Consequently, it indicates the presence of macro-anisotropy in the present geoelectric strata in the area, which is clear to distinguish the individual layers for a given VES earth model[4].

The coefficient of anisotropy shows that it increases from SW to NE and the eastern directions and reaches a maximum value close to 1.9 in the NE direction, as shown in anisotropy map (Figure 6). It indicates that this physical property is not uniform in all directions and anisotropy plays a major role in fracturing. Here it indicates more fracturing towards the NE direction and thus suggests comparatively more potential groundwater zone and hence better prospect for groundwater availability. It is seen that the fracture resistivity map (Figure 7) corroborates with the anisotropy map around the same region in the NE direction and showing low resistivity of the fractured rock. The true resistivity of the fractured rock varies from 10 to 100 Ω.m (Figure 7) and is governed by extent of fracturing, connectivity of fractures as well as the amount of moisture content.

Fracture porosity

To evaluate the water saturation condition of the studied area, the fracture porosity was deduced at 22 sites using coefficient of anisotropy λ values, obtained from the VES geoelectric model parameters. This porosity is associated with tectonic fracturing of rocks and is estimated using the following expression[42]

$$\phi_f = \frac{3.41 \times 10^4 (N-1)(N^2-1)}{N^2 C(\rho_{max} - \rho_{min})}, \quad (6)$$

where ϕ_f is the secondary or fracture porosity, N the vertical anisotropy related to the coefficient of anisotropy λ, ρ_{max} the maximum apparent resistivity (Ω.m), ρ_{min} the minimum apparent resistivity (Ω.m) and C is the specific conductance of groundwater (μS/cm).

The estimates reveal that porosity values increase from SW to NE and the eastern direction in the study area with a maximum value concentrated around the eastern and NE regions as seen in Figure 8. The estimated porosity corroborates with the high and low λ values as seen in Figure 6. This reflects that fracturing is due to anisotropy, and is developed and more prominent in the eastern and SW–NE directions (Figure 6) compared to other parts of the study area. Nevertheless, it also suggests that the fractures are well connected in the eastern and SW–NE directions and indicates that the fractured rock is more likely saturated with water with different degrees of water-holding capacity. This helps in knowing the porosity variation with the rock matrix and in turn hydrogeological scenario of the study area.

Results and discussion

The complete VES data interpretation from a sounding curve is essential, especially in hard-rock terrain for groundwater prospecting and exploration. In the present study coefficient of anisotropy (λ) varies from 1.002 to 1.87, which indicates quite a large variation showing thereby more tendency towards anisotropy behaviour of

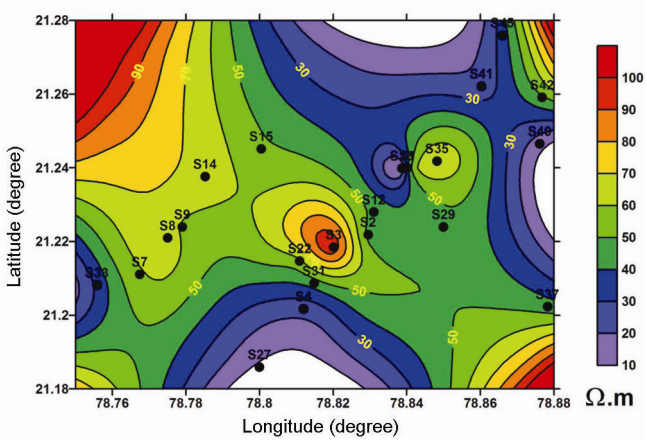

Figure 7. Map showing the fracture resistivity variation in the study area.

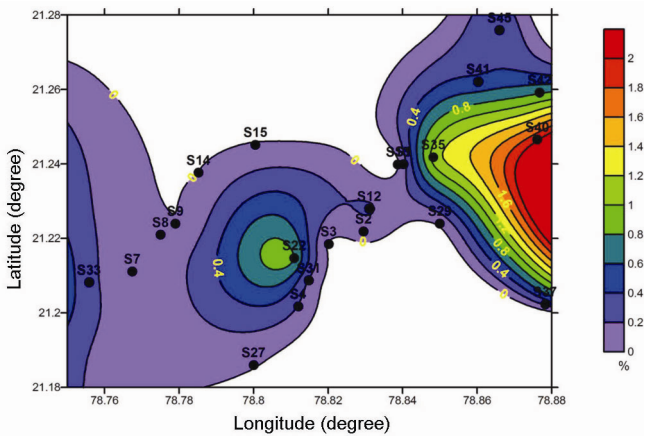

Figure 8. Map showing the fracture porosity variation and its strong correlation with the estimated anisotropy in the study area.

the subsurface geoelectric parameters. In other words, there is large variation in the transverse and longitudinal direction of the weathered/fractured basaltic aquifer in the given study area. The high values of λ ($\lambda > 1$) signify more fracturing within the basaltic rock formation, while values of $\lambda \approx 1$ obtained for basaltic rocks could be explained on the basis of the relatively higher average value of the overburden thickness (H). This can be also witnessed from the plot of aquifer zone thickness and coefficient of anisotropy (Figure 9). Interestingly, λ values increase from SW to NE and in eastern directions with the maximum value concentrated around the eastern and NE parts of the area. It is also uniformly and gradually varying around the eastern part of the area (Figure 6). This clearly indicates that the fractures are more prominent along this direction and are much more developed, which confirms the major role of anisotropy. While on the other hand, the fracture porosity (φ_f) estimate shows equally similar behaviour confirming the highly porous zones in the SW, eastern and NE parts of area (Figure 8),

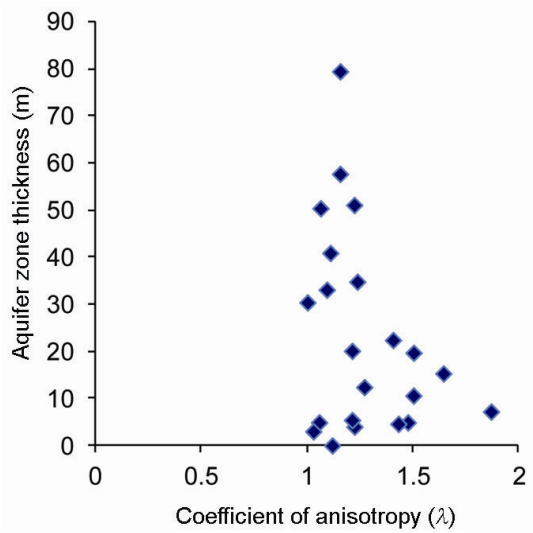

Figure 9. Plot of aquifer zone thickness and coefficient of anisotropy with maximum tendency of anisotropic behaviour of rock mass.

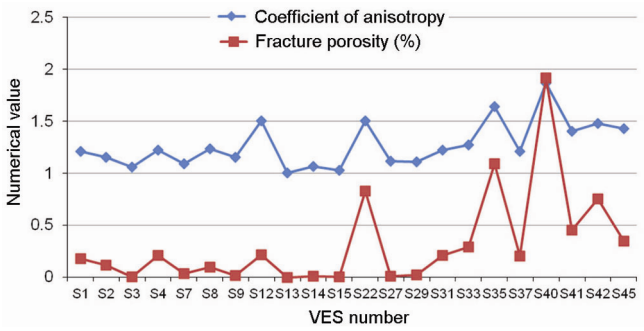

Figure 10. Plot of coefficient of anisotropy (λ) and fracture porosity (φ_f) with VES number depicting λ in most of the cases it is numerically >1.0 showing anisotropy rock mass and a good correlation between them.

which suggests highly saturated fractured and vesicular basalt formations. Such type of basalt normally shows very high porosity values in the Deccan traps[43]. Interestingly, the plot of λ versus φ_f (Figure 10) clearly shows that λ in most of the cases is numerically >1.0, indicating anisotropy rock mass and some values are close to 1.0. The plot shows that the fracture porosity is well corroborated with coefficient of anisotropy. The fracture porosity φ_f varies from 0.007% to ~2%, which suggests different degrees of water saturation in various forms of basaltic rock formation. Nevertheless, a unique example from a 2D inverted resistivity model (Figure 11 *a*) at P1 site near Ghogali village (see Figure 1) is presented here to know the presence of saturated fractured basalt, which is delineated based on the substantial resistivity contrast[44]. It is a clear and distinct zone from the massive basalt. This saturated fractured basalt is confirmed by drilling and the litholog (Figure 11 *b*) depicting the fully saturated fractured and highly fractured basalt – a prosperous and potential aquifer zone. This shows the clear disposition of the aquifer system in the present hard-rock setting. The study exemplifies the high-porosity zone(s), which directly signify large reserves of groundwater in the present geological setting.

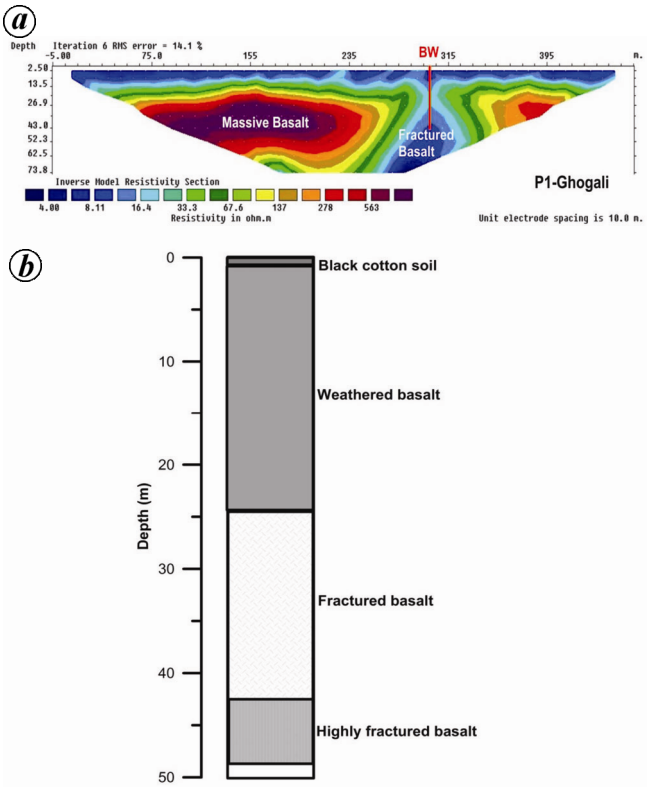

Figure 11. ***a***, Two-dimensional inverted resistivity section at P1 site near Ghogali village confirming prospect and potential aquifer zone with fairly large resistivity contrast between massive and fractured basalt (after Ratna Kumari *et al.*[44]). ***b***, Borehole lithological data at P1 site where the aquifer zone constitutes the fractured and highly fractured basalt formation. Total borewell depth is 48 m.

Conclusions

The detailed characteristics of hard-rock aquifers precisely delineated based on the complete VES resistivity data interpretation using both primary and secondary geoelectric parameters and along with the porosity estimation, gives the direct measure of water saturation of the subsurface rock formation in the present geological setting. The coefficient of anisotropy (λ) varies from 1.002 to 1.87, which indicates large variation showing thereby more tendency towards anisotropy behaviour of the geoelectric parameters of the earth. On the other hand, the fracture porosity φ_f varies from 0.007% to ~2%, showing significant variation and with different degrees of water saturation in fractured/vesicular type of basalts in the area. The high-porosity zones corroborate with the high λ values, signifying large reserves of groundwater. Coincidentally, the fracture resistivity map shows low resistivity (~10–35 Ω.m) indicating water-saturated fracture(s) and it corroborates with the porosity map, especially around the eastern part of the area. The present findings help in quantifying the nature of the fractured rock, distribution of water saturation and characteristics of the geological strata in basaltic hard-rock region.

1. Slater, L. D., Wishart, D. N. and Gates, E. A., Self potential improves characterization of hydraulically active fracture from azimuthal geoelectrical measurements. *Geophys. Res. Lett.*, 2006, **33**, L17314.
2. Skyernaa, L. and Jorgensen, N. O., Detection of local fracture systems by azimuthal resistivity surveys: example from south Norway. In Memoirs of the 24th Congress of International Association of Hydrogeologists, 1993, pp. 662–671.
3. Keller, G. V. and Fischknechst, F. C., *Electrical Methods in Geophysical Prospecting*, Pergamon Press, London, 1966, p. 517.
4. Bhattacharya, P. K. and Patra, H. P., *Direct Current Geoelectric Sounding, Principles and Interpretation, Methods in Geochemistry and Geophysics, Series-9*, Elsevier, The Netherlands, 1968, p. 135.
5. Zohdy, A. A. R., Eaton, G. P. and Mabey, D. R., Application of surface geophysics to groundwater investigation. In *Techniques of Water Resources Investigations*, US Geological Survey, Washington, 1974, p. 116.
6. Watson, K. A. and Barker, R. D., Differentiating anisotropy and lateral effects using azimuthal resistivity offset Wenner soundings. *Geophysics*, 1999, **64**, 749–745.
7. Rao, B. V., Subramanyam, K., Murthy, E. S. R. C., Varalakshmi, V. and Satyanarayana, B., Problems and prospects of geophysical methods in identifying groundwater potential zones of hard rocks. In *Proceedings of the 3rd International Conference on Hydrology and Watershed Management (ICHWAM) with a Focal Theme on Climate Change – Water, Food and Environmental Security*, BS Publication, Hyderabad, 2010, vol. 1, pp. 432–442.
8. Ben, O. I. and Onwuemesi, A. G., Estimation of anisotropic properties of fractures in Presco campus of Ebonyi State University Abakaliki, Nigeria using azimuthal resistivity survey method. *J. Geol. Min. Res.*, 2009, **1**(8), 172–179.
9. Ayolabi, E. A., Olatinsu, O. B. and Badmus, B. S., Groundwater potential evaluation using electrical resistivity method in a typical basement complex area of Nigeria. *J. Sci. Technol.*, 2009, **29**(1), 52–63.
10. Senos Matias, M. J., Square array anisotropy measurements and resistivity sounding interpretation. *J. Appl. Geophys.*, 2002, **49**(3), 185–194.
11. Telford, W. M., Geldart, L. P., Sheriff, R. E. and Keys, D. A., *Applied Geophysics*, Oxford & IBH Publishing, Cambridge, 1976, p. 860.
12. Rai, S. N., Thiagarajan, S., Ratna Kumari, Y., Rao, V. A. and Manglik, A., Delineation of aquifers in basaltic hard rock terrain using vertical electrical soundings data. *J. Earth Syst. Sci.*, 2013, **122**(1), 29–41.
13. Satpathy, B. N. and Kanungo, D. N., Groundwater exploration in hard rock terrain – a case history. *Geophys. Prospect.*, 1978, **2**(4), 725–736.
14. Olorunnlwo, M. A. and Olorunfemi, M. O., Geophysical investigations for groundwater in Precambrian terrains: a case history from Ikare, southwestern Nigeria. *J. Afr. Earth Sci.*, 1987, **8**(6), 787–796.
15. Kumar, D. *et al.*, Groundwater exploration in basaltic formations at Ghatiya Watershed, Madhya Pradesh: an integrated study. Technical Report No. NGRI-2008-GW-632, NGRI, Hyderabad, 2008.
16. Kumar, D., Rao, V. A., Nagaiah, E., Raju, P. K., Mallesh, D., Ahmeduddin, M. and Ahmed, S., Integrated geophysical study to decipher potential groundwater and zeolite-bearing zones in Deccan Traps. *Curr. Sci.*, 2010, **98**(6), 803–814.
17. Krishnamurthy, N. S., Kumar, D., Negi, B. C., Jain, S. C., Dhar, R. L. and Ahmed, S., Electrical resistivity investigations in Maheswaram Watershed, Andhra Pradesh, India. Technical Report No. NGRI-2000-GW-287, NGRI, Hyderabad, 2000.
18. Kumar, D., Ahmed, S., Prakash, B. A. and Krishnamurthy, N. S., Combined use of geological logs and vertical electrical soundings (VES) for spatial prediction of weathered rock thickness and depth to bedrock in an aquifer. In *Proceedings of the International Groundwater Conference (IGC-2002) on Sustainable Development and Management of Groundwater Resources in Semi-Arid Region with Special Reference to Hard Rocks*, Oxford and IBH Publishing, 2002, pp. 383–390.
19. Krishnamurthy, N. S., Kumar, D., Ananda Rao, V., Jain, S. C. and Ahmed, S., Comparison of surface and subsurface geophysical investigations in delineating fracture zones. *Curr. Sci.*, 2003, **84**(9), 1242–1246.
20. Kumar, D., Conceptualization and optimal data requirement in simulating flow in weathered–fractured aquifers for groundwater management, Ph.D. thesis, Osmania University, Hyderabad, 2004, p. 213.
21. Kumar, D., Ahmed, S., Krishnamurthy, N. S. and Dewandel, B., Reducing ambiguities in vertical electrical sounding interpretations: a geostatistical application. *J. Appl. Geophys.*, 2007, **62**(1), 16–32.
22. Rai, S. N., Thiagarajan, S. and Ratnakumari, Y., Exploration for groundwater in the basaltic Deccan Traps terrain in Katol Taluk, Nagpur district, India. *Curr. Sci.*, 2011, **101**(9), 1–8.
23. Sen, A. K. and Ghatak, S. K., Report on the geophysical investigations for groundwater in water scarcity affected villages of Nagpur district, Maharashtra. GSI, Central region, 1983, p. 8.
24. Murthy, B. V. S., Mohammed, G. and Sitaramaiah, S., An objective approach to mineral exploration through geophysical mapping – a study of Pakhal Cuddapah tract of AP, India. *Geophys. Res. Bull.*, 1983, **21**, 113–129.
25. Murthy, B. V. S., Bhimasankaram, V. L. S. and Varaprasada Rao, S. M., Structure and geology from Maneru valley from gravity and magnetic surveys. *Indian Acad. Geosci.*, 1984, **24**, 5–12.
26. Muralidharan, D., Deshmukh, S. D., Rangarajan, R., Krishna, V. S. R. and Athavale, R. N., Deep resistivity surveys for delineation of Deccan Trap–Gondwana contact and selection of water-well sites in Jam River Basin. Technical Report No. NGRI 1994-GW-153, NGRI, Hyderabad, 1994, p. 1–63.

27. Chandra, S., Ananda Rao, V. and Singh, V. S., A combined approach of Schlumberger and axial pole–dipole configurations for groundwater exploration in hard rock areas. *Curr. Sci.*, 2004, **86**(10), 1437–1443.
28. Yadav, G. and Singh, S. K., Gradient profiling for the investigation of groundwater saturated fractures in hard rocks of Uttar Pradesh, India. *Hydrogeol. J.*, 2007, **16**(2), 363–372.
29. Chakravarthi, V., Shankar, G. B. K., Muralidharan, D., Harinarayana, T. and Sundararajan, N., An integrated geophysical approach for imaging sub basalt sedimentary basins: case study of Jam River basin, India. *Geophysics*, 2007, **72**(6), B141–B147.
30. Jha, Madan, K., Kumar, S. and Chowdhury, A., Vertical electrical sounding survey and resistivity inversion using genetic algorithm optimization technique. *J. Hydrol.*, 2008, **359**(1–2), 71–87.
31. Mondal, N. C., Das, S. N. and Singh, V. S., Integrated approach for identification of potential groundwater zones in Seethanagaram Mandal of Vizianagaram District, Andhra Pradesh, India. *J. Earth Syst. Sci.*, 2008, **117**(2), 133–144.
32. Mehta, M., Groundwater resources and development potential of Nagpur district, Maharashtra. Report of Central Groundwater Board, India, 1989, 434/DR/12/89.
33. Orellana, E. and Mooney, H. M., *Master Tables and Curves for Vertical Electrical Sounding Over Layered Structures*, Interciencia, Madrid, Spain, 1966.
34. Rijkswaterstaat, Standard graphs for resistivity prospecting. European Association of Exploration Geophysicists, Hague, The Netherlands, 1969.
35. Zohdy, A. A. R., The auxiliary point method of electrical sounding interpretation and its relationship to Dar Zarrouk parameters. *Geophysics*, 1965, **30**(4), 644–660.
36. Van Der Velpen, RESIST, version 1.0, a package for the processing of the resistivity sounding data. M Sc Research Project, International Institute for Aerospace Survey and Earth Observation Dept, The Netherlands, 1988.
37. Maillet, R., The fundamental equations of electrical prospecting. *Geophysics*, 1947, **2**, 529–556.
38. Galin, D. L., Use of longitudinal conductance in vertical electrical sounding induced potential method for solving hydrogeologic problems. *Vestrik Moskovskogo Univ. Geol*., 1979, **34**, 74–100.
39. Henriet, J. P., Direct application of the Dar-Zarrouk parameters in groundwater surveys. *Geophys. Prospect.*, 1976, **24**, 344–353.
40. Kalenov, E. N., *Interpretation of Vertical Electrical Sounding Curves*, Gostoptekhiz, Moscow, 1957, p. 412.
41. Kuentz, G., *Principles of Direct Current Resistivity Prospecting*, Grebruder Bokrntraeger, Berlin, 1966, p. 103.
42. Lane Jr, J. W., Haeni F. P. and Watson, W. M., Use of a square-array direct current resistivity method to detect fractures in crystalline bedrock in New Hampshire. *Groundwater*, 1995, **33**(3), 476–485.
43. Deolankar, S. B., The Deccan basalt of Maharashtra, India – their potential as aquifers. *Groundwater*, 1980, **18**(5), 434–437.
44. Ratna Kumari, Y., Rai, S. N., Thiagarajan, S. and Kumar, D., 2D electrical resistivity imaging for delineation of deeper aquifers in parts of Chandrabhaga river basin, Nagpur district, Maharashtra, India. *Curr. Sci*., 2012, **102**(1), 61–69.

ACKNOWLEDGEMENTS. We thank Prof. Mrinal K. Sen, former Director NGRI, Hyderabad for his kind consent and encouragement to publish this research work. We also thank CSIR, New Delhi for providing the Network Project on Groundwater during the 11th Five-Year Plan and financial support for carrying out a major research project on groundwater studies in problematic areas of the hard rock terrain in the country and the anonymous reviewers for their valuable comments that helped improve the manuscript.

Received 25 April 2014; accepted 11 July 2014